Development 140, 1137-1146 (2013) doi:10.1242/dev.087734
© 2013. Published by The Company of Biologists Ltd

Pseudotyped retroviruses for infecting axolotl *in vivo* and *in vitro*

Jessica L. Whited[1], Stephanie L. Tsai[1,2], Kevin T. Beier[1,3], Jourdan N. White[1], Nadine Piekarski[4], James Hanken[4], Constance L. Cepko[1,3,5] and Clifford J. Tabin[1,*]

SUMMARY

Axolotls are poised to become the premiere model system for studying vertebrate appendage regeneration. However, very few molecular tools exist for studying crucial cell lineage relationships over regeneration or for robust and sustained misexpression of genetic elements to test their function. Furthermore, targeting specific cell types will be necessary to understand how regeneration of the diverse tissues within the limb is accomplished. We report that pseudotyped, replication-incompetent retroviruses can be used in axolotls to permanently express markers or genetic elements for functional study. These viruses, when modified by changing their coat protein, can infect axolotl cells only when they have been experimentally manipulated to express the receptor for that coat protein, thus allowing for the possibility of targeting specific cell types. Using viral vectors, we have found that progenitor populations for many different cell types within the blastema are present at all stages of limb regeneration, although their relative proportions change with time.

KEY WORDS: Axolotl, Regeneration, Retrovirus, Tissue specific

INTRODUCTION

Among vertebrates, salamanders exhibit the most remarkable regenerative abilities – many species can replace limbs and tails (among other structures) even as adults (reviewed by Brockes and Kumar, 2005). Although the biological processes underlying this remarkable regenerative ability have been investigated for decades, a mechanistic understanding at a genetic or molecular level has remained elusive, owing in large part to a lack of modern tools that can be applied to salamanders (reviewed by Whited and Tabin, 2009). Transgenesis is possible (Sobkow et al., 2006) but is relatively inefficient, suffers from the long generation time of the axolotl, and has only recently been coupled with any induction system (Whited et al., 2012) or tissue-specific promoters (Monaghan and Maden, 2012). Electroporation is currently the predominant means with which to mis-express genetic elements in salamanders (Berg et al., 2010; Echeverri and Tanaka, 2002; Echeverri and Tanaka, 2003; Echeverri and Tanaka, 2005; Kumar et al., 2007; Mercader et al., 2005), yet this method has drawbacks, such as dilution of plasmid with cell division, and the procedure itself has been shown to cause some degree of cellular de-differentiation in newts (Atkinson et al., 2006) akin to the de-differentiation that is a hallmark of limb regeneration.

Viral gene transfer is an attractive alternative, as it can provide stable gene expression and can, in principle, be targeted to specific cell types based on the availability of a receptor. Pseudotyped retroviruses, in which viral particles are coated by ectopic envelopes to expand their host range, have previously been used to introduce foreign DNA into newt cells in culture, and these infected cells have been implanted into regenerating limbs (Cash et al., 1998; Kumar et al., 2000). One study infected regenerating axolotls with Vaccinia (Roy et al., 2000), but no additional studies have used Vaccinia, perhaps because of the its large and difficult-to-engineer genome. We have found that pseudotyped Maloney Murine Leukemia Virus (MMLV) retroviruses can very efficiently infect axolotl cells *in vitro* and *in vivo*, and can be used for both lineage and functional analyses in regenerating limbs. When these retroviruses are pseudotyped with ASLV-A envelope glycoprotein that mediates infection specifically through the avian TVA receptor, they are capable of infecting only axolotl cells that have been made to express the receptor. These technical advances expand the toolkit available to axolotl researchers.

MATERIALS AND METHODS

AL1 cell culture

AL1 cells were maintained and transfected as previously described (Lévesque et al., 2007).

Constructs

A retroviral vector was based pQCXIX vector (Clontech). It was modified to contain EGFP upstream of the IRES, generating pQC-EGFP (pCMV-EGFP). Further modification replaced CMV promoter with CAG [CMV enhancer, chicken β-actin promoter, β-actin and β-globin introns; gifts from C. Punzo (University of Massachusetts Medical School, Worcester, MA, USA) and C. Cepko (Harvard Medical School, Boston, MA, USA)] creating pQCAG-GFP. pCAG-TVA is described elsewhere (Beier et al., 2011). pPECAM-EGFP [Addgene #14688 (Kearney et al., 2004)] was modified by ligating an oligo with a *Not*I site into the *Sac*II site between PECAM and EGFP; EGFP was excised with *Not*I replaced with TVA to create pPECAM-TVA.

Virus production

Virus was produced as described previously (Beier et al., 2011). Titers for viruses produced using this protocol were between 10^7 and 10^8 infectious particles/ml. Modifications were made to produce high-titer virus (10^8-10^9 infectious particles/ml). Constructs were transfected into 293T cells on poly-D-lysine-coated plates (10 cm) ~80% confluency. For each of the 12 plates, 250 µl DMEM, 25 µl PEI (1 mg/ml) and plamsids [6 µg pQ-(X), 3 µg helper (encoding gag/pol) and 1 µg encoding coat protein] were mixed, incubated

[1]Department of Genetics, Harvard Medical School, 77 Avenue Louis Pasteur, Boston, MA 02115, USA. [2]Department of Biology, Massachusetts Institute of Technology, 77 Massachusetts Avenue, Cambridge, MA 02142, USA. [3]Howard Hughes Medical Institute, Harvard Medical School, Boston, MA, 02115, USA. [4]Department of Organismal and Evolutionary Biology, Harvard University, Cambridge, MA 02138, USA. [5]Department of Ophthalmology, Harvard Medical School, 77 Avenue Louis Pasteur, Boston, MA 02115, USA.

*Author for correspondence (tabin@genetics.med.harvard.edu)

Accepted 14 December 2012

(for 15 minutes at room temperature), and added to cells with fresh media. Media were replaced the following day with 5 ml 10% Nu serum media, collected the following 2 days, yielding 120 ml total/virus. Media/virus were frozen at −80°C. Thawed virus was concentrated by centrifugation with Centricon Plus-70 filters (Millipore) followed by ultracentrifugation. The supernatant was discarded and tube walls were aspirated leaving ~50 μl, which was incubated overnight at 4°C then gently shaken at 4°C the following day, aliquotted and stored at −80°C.

Viral infection of AL1 cells

AL1 cells can be infected by adding concentrated virus to their ordinary media [culture conditions have been described previously (Lévesque et al., 2007)]. When maximizing infection, cells were plated in 24-well plates (split 1:2 from a confluent culture), media were replaced the following day with 100 μl fresh media, virus (1-2 μl) was added, the cells were incubated for 2 hours, then 300 μl media added. For viral infections of AL1 cells transfected via electroporation, we waited several days for cells to settle and serum was increased to 10% to help stimulate recovery and proliferation.

Viral infection of animals

Infections were performed while animals were anesthetized. Capillary needles were back-filled with virus/Fast Green solution, and tissues were filled with virus using a pneumatic device; later-staged blastemas required larger volumes of virus (up to 1.5 μl), whereas earlier-staged blastemas required less virus (~0.5 μl).

Skeletal preparations

Alcian Blue staining was performed as described previously (Whited et al., 2012).

Histology

Limbs were processed as described previously (Whited et al., 2011). Cryosections were rehydrated in PBS, blocked in PBS/2% BSA/0.1% Triton for 30 minutes, incubated in primary antibody (chicken anti-GFP, 1:1000, Abcam), washed three times in PBS for 5 minutes and incubated in secondary antibody (donkey anti-chick or goat anti-chick, AlexaFluor 488-conjugated, 1:250, Jackson Labs). Incubations were 2-4 hours at room temperature or overnight at 4°C. Where indicated, sections were counterstained with AlexaFluor 594 phalloidin (1:40 with secondary antibody) and DAPI. Slides were mounted with Prolong Gold and imaged on a Zeiss LSM780 inverted confocal microscope. In Fig. 5D-F, we used Cy3-conjugated goat anti-chick (Jackson Labs) to image EGFP in a red channel and Abcam ab8211 FITC-conjugated anti-α smooth muscle actin.

Animals

Experimentation was in accordance with Harvard University's Institutional Animal Care and Use Committees (IACUC). Animals were bred in-house or obtained from the Ambystoma Genetic Stock Center (AGSC) (Lexington, KY) and were between 6 and 12 cm long and size-matched within experiments, except where noted. Amputations were performed as described previously (Whited et al., 2011).

RESULTS

Broad retroviral infections *in vitro* and *in vivo*

For a viral vector to be useful in driving expression of foreign DNA in target cells, it must gain entry into those cells and contain a promoter capable of driving high levels of gene expression in the cell type being infected. Previous studies with regenerating and cultured newt cells indicated that Malony Murine Leukemia Virus (MMLV) could be engineered to infect these amphibian cells if the virus were 'pseudotyped' such that it was encompassed in the coat of a virus with a wider host range, in particular, carrying the G protein of vesicular somatitis virus (VSV) (Burns et al., 1994; Cash et al., 1998). These retroviruses are capable only of infecting mitotically active cells, as breakdown of the nuclear envelope is required for the viral genome to integrate into the host. Thus, they can be used to target cells currently undergoing mitosis among a mixture of mitotic and non-mitotic cells. As a starting point, we adopted the VSV-G-pseudotyping strategy for infecting axolotl cells. To drive gene expression, we took advantage of previous studies showing that the well-characterized CAG promoter (Niwa et al., 1991) works well in axolotl cells (Kawakami et al., 2006; Sobkow et al., 2006). Accordingly, we used an MMLV vector in which the strong endogenous retroviral LTR promoter is self-inactivated during the reverse-transcriptase step of infection of the host cell (making use of a promoter mutation in the 3′ LTR), thus allowing efficient use of an internal promoter (Yu et al., 1986), such as CMV or CAG. While we reasoned that the resulting vectors, QCMV and QCAG, might provide genetic access to all mitotically active cells in a regenerating axolotl limb, the same strategy could in principle be used with tissue-specific promoters inserted into the same vector backbone to target specific cell types. We found that the CMV viruses produced similar results to those with a full CAG promoter *in vivo*.

Initially, we used axolotl AL1 cells to test the capabilities of the pseudotyped QCMV virus *in vitro*. We followed infection with EGFP encoded downstream of the CMV promoter in the viral vector. AL1 cells are an apparently immortal cell line derived from mature axolotl limb tissue (Roy et al., 2000). We found VSV-pseudotyped QCMV-GFP was indeed capable of infecting AL1 cells (Fig. 1A,B) when cells were infected with a 1:500 dilution of a 10^8 titer virus and imaged 10 days later. To examine the efficiency and kinetics of retroviral infection *in vitro*, we infected cells with ~600,000 QCMV-GFP virions/ml. Within five days post infection, a subset of cells could be seen as faintly – but unambiguously – GFP positive. One week post infection, small clones (usually one-two cells) of fluorescent cells were evident, with ~10% of cells expressing GFP (supplementary material Fig. S1A,A′). Three weeks post-infection, we found 13% of cells to be GFP positive (supplementary material Fig. S1B,B′). Infections generally produced two-cell clones within 1 week post-infection and four-cell clones within 2 weeks post-infection. This rate of cell division *in vitro* is consistent with the proliferation of AL1 cells, which when split 1:2 require 1 week to reach confluency, in stark contrast to most of the mammalian cell lines (for example, 293T cells), which divide much more quickly. To optimize infection, we used the same virus media volume (see Materials and methods), and we found that we could achieve 50% infectivity (scored 6 days post-infection). A higher titer (2×10^9) of the virus resulted in an increased percentage of infected AL1 cells (>80%). The infection of axolotl AL1 cells *in vitro* with the QC retroviruses suggested that infection *in vivo* may be possible and that we may expect to see increased efficiency of infection as target cells can be directly exposed to concentrated virus and many cell types might be dividing more rapidly than AL1 cells (e.g. the highly proliferative blastema cells).

We next tested the ability of the VSV-pseudotyped QCMV virus to infect mitotically active axolotl cells *in vivo*. Axolotls are an important model organism for understanding vertebrate development; hence, we injected the virus into specific locations within developing embryos to target specific progenitor pools. The embryonic anterior neural tube (Fig. 1C) was injected, thus infecting the presumptive head neural crest (Epperlein et al., 2000). Additionally, the paraxial mesoderm was targeted through injection. Neural crest cells migrate from the dorsal neural tube and give rise to a range of well-characterized cell types (see Hanken and Gross, 2005). Fourteen embryos were injected with the virus and six survived to hatchling stage; all six showed GFP fluorescence in live animals and were used for more detailed

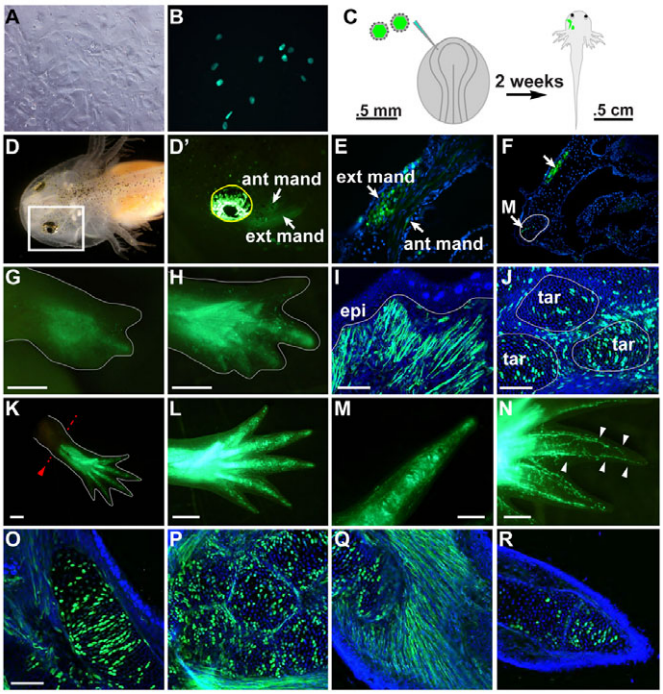

Fig. 1. VSV-G-psuedotyped QC retroviruses can infect axolotl cells *in vitro* and *in vivo*. (**A**,**B**) Axolotl AL1 cells were infected with VSV-G-pseudotyped QCMV-nls-EGFP. (A) Bright-field DIC. (B) Green channel shows cells descended from infected cells. (C-F) Cranial neural crest and underlying mesenchymal cells in axolotl embryos (stage 16) were infected with VSV-G-psuedotyped QCMV-EGFP, and their descendants were tracked when the animals reached hatchling stage. (**C**) Schematic for infections. (**D**,**D′**) Bright-field and fluorescent images of the head of an infected animal. The eye (outlined in yellow) is autofluorescent. (**E**) Transverse section of specimen pictured in D,D′ shows EGFP-expressing cells in the head muscles mm. levator mandibulae anterior (ant mand) and levator mandibulae externus (ext mand). Sections are stained with anti-GFP (green) and DAPI (blue). (**F**) Transverse section of the same specimen more caudally documenting EGFP$^+$ cells in the mesoderm-derived m. levator mandibulae externus (ext mand, top arrowhead) and in the neural crest-derived Meckel's cartilage (M). (**G**) Regenerating hind limb of live animal expressing EGFP 5 days after infection with QCMV-EGFP. (**H**) The same limb as in G, 11 days post-infection. (**I**,**J**) Cryosections of limb shown in G and H, harvested 11 days post-infection, 27 days post-amputation, stained with anti-GFP (green) and DAPI (blue). (I) In the posterior mesenchyme just beginning to undergo condensation to form digits, the majority of the overlying cells (both undifferentiated mesenchymal cells and nascent muscle fibers) are EGFP$^+$. The epidermis (epi) is negative. (J) Condensations forming the tarsals (tar, outlined) have ~46% EGFP$^+$ cells, whereas ~62% of intervening joint cells are EGFP$^+$. (**K**) After full regeneration (unfixed, freshly harvested at 7 weeks post-amputation), limbs whose blastemas were infected at 2 weeks post-amputation show very robust EGFP fluorescence in many tissues distal to the amputation plane (dotted line) and no fluorescence more proximally. (**L**) Higher magnification view of autopod from limb shown in K. (**M**) Chondrocytes in a live limb. (**N**) Labeled vasculature (arrowheads) in the digits of a limb whose blastema was infected 3 weeks post-amputation. (**O-R**) Cryosections from the limb shown in K,L show a high percentage of infected cells in various tissues. (O) Distal tibia. (P) Tarsal cartilages and joint tissue. (Q) Muscle. (R) Digit tip. Scale bars: 1 mm in G,H,K,L; 200 μm in I,J,O-R; 500 μm in M,N.

analysis (cryosections and antibody stains). As expected, infected neural crest cells and mesoderm cells in the embryo were seen to give rise to skeletal elements in the head, muscles and connective tissue (Fig. 1D-F′).

Next, we tested the QCMV-EGFP virus in regenerating limbs. Limbs were amputated mid-humerus or mid-femur and blastemas were infected with virus 2 weeks later (titer 6×10^8). We found freshly concentrated virus gave the most robust infections, though frozen/thawed aliquots also infected many cells. By 5 days post-infection, all infected limbs showed EGFP fluorescence under a fluorescent stereodissection microscope (n=16, Fig. 1G). One week later, the fluorescence had intensified and expanded (Fig. 1H), presumably owing to accumulation of EGFP and proliferation of descendants of infected cells. Cryosections through regenerating limbs at this point (27 days post-amputation, 11 days post-infection) revealed in the least differentiated tissues (for example, the posterior autopod where digits have not yet formed), a large fraction of cells were labeled (Fig. 1I). More proximally, ~46% of tarsal cartilage cells were labeled (n=72/157), and 62% of cells of joint cells between condensed cartilage were labeled (n=57/92, Fig. 1J). Approximately 19% (n>400) of tibia and fibia cartilage cells were labeled. When limbs were fully regenerated (6 weeks post-amputation), all limbs (n=7) infected with this virus showed robust EGFP expression throughout the regenerated region of the limb (Fig. 1K,L), with many identifiable cell types in live animals, including muscle fibers (for example, the nascent muscle fibers in Fig. 1H and the very bright EGFP expression in swaths of Fig. 1L), chondrocytes (Fig. 1M), vasculature (Fig. 1N, infected 3 weeks post-amputation), and joint cells (supplementary material Fig. S2). Cryosections revealed ~40% of tibia cells (Fig. 1O), 42% of tarsal cartilage cells and many of the joint cells between them (Fig. 1P), the vast majority of the overlying muscle (Fig. 1Q), and 33% of digit tip chondrocytes expressed the marker.

Retroviruses can be used to fate map descendants of mitotically active blastema cells

To investigate the fate of blastema cells at various stages of regeneration, we infected blastemas at various time points post-amputation with a lower titer virus (10^7) (Fig. 2A). Limbs were harvested at 7 weeks post-amputation (for example, Fig. 2B infected with 10^8 QCMV-EGFP), cryosectioned, stained with anti-GFP, DAPI and phalloidin to evaluate the types of cells that were descended from the blastema cells (for example, Fig. 2C). We used an antibody to GFP on sections infected with QCMV-EGFP and QCMV-Venus to ensure all labeled cells would be detected. Based on location and morphology, a large fraction of labeled cells in regenerating blastemas infected with QCMV-VENUS were chondrocytes, including resting, proliferating and hypertrophic chondrocytes (Fig. 2D-F). However, many other cell types were also detected, including perichondrial cells (Fig. 2F), joint cells (Fig. 2G), muscle cells (Fig. 2H), dermal fibroblasts (Fig. 2I) and vascular cells (Fig. 2J-J″). We did not observe any infected epidermal cells. These results are consistent with successful infection of a wide range of progenitor cells within blastemas. Late infections often displayed lower numbers of marked cells within a patch, probably owing to the decreased amount of proliferation that has occurred between infection and harvest compared with earlier infections (for example, two small mother/daughter pairs are seen in the distal phalange shown in Fig. 2G). We did not observe any labeled neurons, consistent with the fact that the MMLV retroviruses do not infect post-mitotic cells.

As the QC vector lacks the endogenous viral genes *gag*, *pol* and *env*, and has a self-inactivating LTR, it is incapable of spreading from the initially infected cells. Thus, infection serves to mark the cells and (as the virus integrates its genome into the host DNA) direct descendants of the infected cell. This property, being a

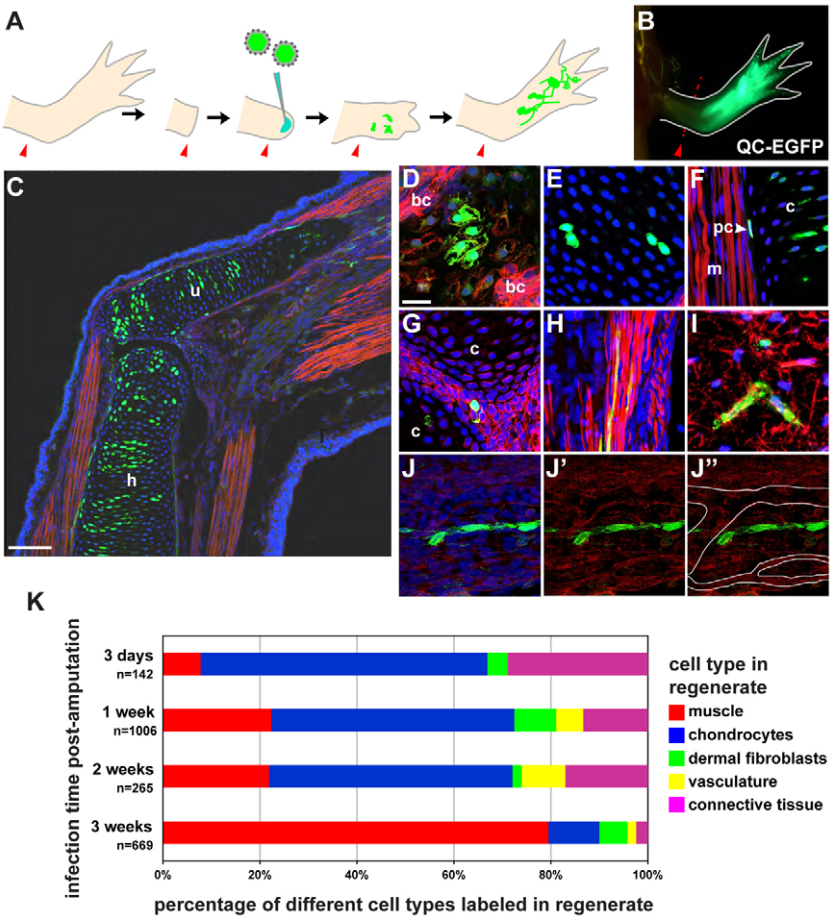

Fig. 2. Infection of blastemas at various time points post-amputation reveals progenitors for nearly every cell type are present in the blastema and are mitotically active throughout regeneration. (**A**) Schematic of experiment. Limbs were amputated at mid-stylopod (mid-humerus for forelimbs, mid-femur for hindlimbs) (arrowheads). Blastemas were infected with a VSV-G pseudotyped-, replication-incompetent QCMV retrovirus encoding a fluorophore, and limbs were harvested after full regeneration. (**B**) Example of an infection as performed in the schematic. (**C**) Regenerated forelimb infected with QCMV-EGFP 12 days post-amputation, cryosectioned and stained with anti-GFP (green), AlexaFluor-594-conjugated phalloidin (red) and DAPI (blue). Scale bar: 250 μm. h, humerus; u, ulna. (D-J″) High-magnification views of cell types identified when blastemas were infected with QCMV-Venus and regenerated limbs stained as in C. Scale bar: 50 μm. (**D**) Hypertrophic chondrocytes (bc, bone collar). (**E**) Two pairs of mother/daughter chondrocyte pairs in a distal phalange. (**F**) Perichondrial cell (pc) (adjacent muscle marked 'm' and cartilage 'c'). (**G**) A single marked joint cell between two carpals (c). (**H**) Muscle fibers. (**I**) Dermal fibroblasts. (**J-J″**) A string of labeled vasculature cells within a capillary bed. (J) All three channels. (J′) DAPI channel subtracted for better visualization of unlabeled vessels, apparent by their F-actin organization. (J″) Adjacent and intersecting vessels outlined. (**K**) Relative proportion of descendant cell types at various infection times. Total numbers of cells counted for each time point are given below *y*-axis labels.

permanent yet non-spreading marker, allowed us to use the virus to survey the lineage of mitotic blastema cells at various stages of limb regeneration. Recent studies have indicated that blastemas are a heterogeneous population of tissue-specific progenitor cells rather than a population of a single type of multipotent stem cell (Kragl et al., 2009). However, it has not been tested whether progenitors within the blastema are equivalent throughout the regenerative process. For example, in the retina, although there are multiple classes of progenitor cells present at any given time of development, different retinal cell subtypes are born at different times (Rapaport et al., 2004; Sidman, 1961; Young, 1985a; Young, 1985b). In regeneration, it was possible that different tissue-specific progenitors could be induced to enter the blastema from the stump at different time points. To examine the temporal profile of progenitors within the blastema, early- (3 days post-amputation), mid- (1 and 2 weeks post-amputation) and late-staged (3 weeks post-amputation) blastemas were infected. Fig. 2K summarizes the data. In all cases, we found muscle, cartilage, connective tissue (joint, perichondrial and tendon cells) and fibroblast cell types fluorescent in the regenerate, indicating that progenitors for these lineages are present and mitotically active in the blastema at all time-points assayed. We found labeled vascular cells descended from all infection times assayed, except the earliest time point, 3 days post-amputation.

Retroviruses for misexpressing functional molecules during regeneration

To determine whether these pseudotyped MMLVs might be useful for mis-expressing genetic elements during limb regeneration, we engineered a QCAG virus to contain the chicken Sonic Hedgehog-coding region. We infected regenerating limbs with this QCAG-SHH virus and examined fully regenerated limbs for evidence that mis-expressed SHH protein perturbed patterning. Skeletal preparations from uninfected limbs show a precise configuration of carpal and tarsal elements in the wrist and ankle joints, respectively (*n*=42/42, Fig. 3A,A′,D,D′) as do skeletons of limbs infected with QCMV-EGFP (*N*=15/16). A large fraction of the QCAG-SHH-infected limbs contained ectopic and/or fused central elements in wrist and ankle (*n*=16/20, Fig. 3B-C′,E,E′), demonstrating that these viruses may be useful tools for assessing gene function during regeneration.

Axolotl cells ectopically expressing TVA receptor can be infected by ASLV-A pseudotyped retroviruses

Using viral infection as a tool for examining the range of progenitors present in the blastema required the virus infect a broad spectrum of cell types. Such broad tropism was achieved by pseudotyping the QC vectors with VSV-G (Lois et al., 2002). However, MMLV can be pseudotyped with foreign coat glycoproteins that enable more restricted tropisms, such as the ASLV-A glycoprotein, which permits infection of only TVA-receptor (TVA)-expressing cells (Young et al., 1993). The TVA receptor is found on the surface of certain avian cells, but is not present in axolotl cells (as judged by our inability to infect axolotl AL1 cells with an avian-based retrovirus in preliminary studies). Thus, we reasoned that ectopically expressing TVA in axolotl cells could render a subset of cells infectable by virus pseudotyped with ASLV-A. Similar

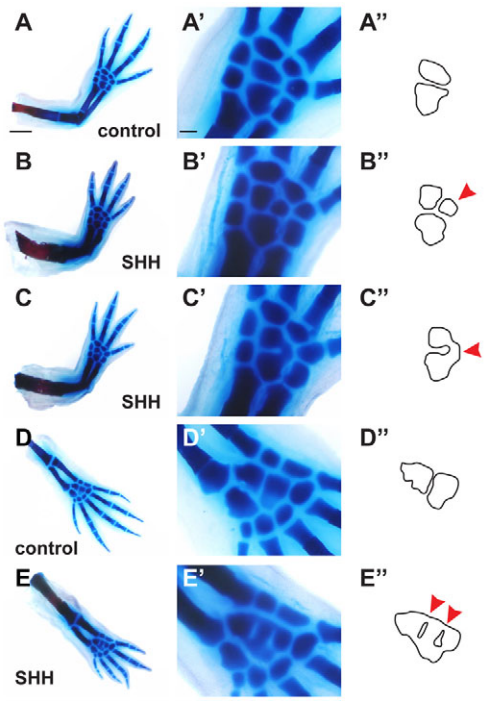

Fig. 3. Regenerating limbs infected with QCAG-SHH have defective skeletal structures. (**A**) Uninfected control forelimb showing normal skeletal morphology. (**A′**) Higher-magnification view of carpals. (**A″**) Outline of central carpal elements. (**B-C″**) Regenerating forelimbs infected with QCAG-SHH show abnormal skeletal patterning following regeneration. (B-B″) Ectopic central carpal (arrowhead). (C-C″) Fusion between top and bottom central carpals (arrowhead). (**D-D″**) Uninfected control hindlimb including outline of central tarsal elements. (**E-E″**) Hindlimb infected with QCAG-SHH during regeneration showing ectopic tarsals/tarsal fusion (arrowheads). Scale bars: 1 mm in A-E; 200 μm in A′-E′.

strategies have been extensively employed in mammals (Federspiel et al., 1994; Lewis et al., 2001; Young et al., 1993). To test this, we transfected AL1 cells with a construct encoding TVA under the control of ubiquitously active CAG promoter and a co-electroporation control plasmid. We used an optimized infection protocol. As expected, control cells that were electroporated with only pCAG-EGFP were never infected by the ASLV-A pseudotyped QCMV-H2B-mRFP virus (titer 10^9) (Fig. 4A,A′). Nearly all the cells surviving the electroporation procedure were EGFP$^+$ (n>1000 cells) and none appeared to express RFP; we counted cells under the 10× objective and found all 464 EGFP$^+$ cells examined were negative for RFP. By contrast, cells electroporated with both pCAG-EGFP and pCAG-TVA were susceptible to infection with ASLV-A pseudotyped QCMV-H2B-mRFP (Fig. 4B,B′, 4 days post-infection). Under the 10× objective, we located easily countable groups of EGFP$^+$ cells. We found that 156 of 166 GFP$^+$ cells examined had mRFP$^+$ nuclei, indicating that at ~94% of TVA-expressing cells were infected with the ASLV-A pseudotyped QCMV-H2B-mRFP virus. Many cells were both intensely green and red. Among the double-positive cells, we found examples of cells with both intense EGFP expression and mild RFP expression and vice versa (Fig. 4C,C′). This latter class of cells illustrates that few TVA molecules are likely to be necessary to mediate infection by ASLV-A pseudotyped retroviruses. We observed similar results with other fluorophore marker configurations.

We extended these results *in vivo* by performing a similar experiment in regenerating limbs. In preliminary experiments, blastemas electroporated with pCAG-TVA (either 7 or 14 days post-amputation) and infected with 10^7 titer ASLV-A-pseudotyped QCAG-EGFP virus 3 days later showed small patches of EGFP$^+$ cells after full regeneration (n=6/8). We extended this result by performing a similar experiment using higher titer (10^9) virus (Fig. 4D-F). Blastemas electroporated with only pCAG-H2B-EGFP and injected with ASLV-A-pseudotyped QC-H2BmRFP showed expression of EGFP but not mRFP (Fig. 4D,D′, n=8). By contrast, blastemas electroporated with pCAG-H2B-EGFP and pCAG-TVA and injected with the same virus showed expression of both EGFP and mRFP (Fig. 4E,E′, n=8) at 10 days post-infection, indicating that axolotl limbs need to be supplied with TVA to become infected. To quantify infection, we cryosectioned limbs and analyzed them. The total number of cells infected can be expected to be a direct reflection of several factors, notably the number of cells expressing the TVA, which is a function of the electroporation efficiency. Because of varying efficiency and plasmid dilution with cell division, we quantified the number of infected cells within a patch of electroporated cells 1 week post-electroporation and 5 days post-infection rather than quantifying after full regeneration in which dilution of electroporation marker would make reliable identification of descendants from electroporated cells impossible. We cloned the TVA cDNA into an expression vector that would allow both the TVA receptor and the fluorescent marker to be expressed from the same plasmid (pCMV-TVA-2A-tdTomato), eliminating the possibility that some cells would be transfected with DNA encoding TVA but not the fluorescent marker, and vice versa. Limbs electroporated with pCMV-TVA-2A-tdTomato were infected with ASLV-A-pseudotyped QCMV-EGFP. We found 80% (235/294) of cells expressing tdTomato also expressed the viral marker under these conditions. If late-stage blastemas are electroporated (24 days post-amputation) and infected (7 days post-electroporation), and limbs allowed to regenerate fully, the infected patches always co-exist within a domain of electroporated cells of the same cell type (Fig. 4H-I″), a result that would be expected if these late-stage blastema cells are largely committed to cell type and location. We never observed patches of infected cells in locations distant from co-electroporation markers, consistent with axolotl cells needing to be supplied with a way to express TVA in order to become infected. Using this electroporation/infection strategy, we observed a variety of cell types in the regenerated limb expressing the viral marker, for example, joint cells (Fig. 4J), chondrocytes (Fig. 4K), muscles (Fig. 4L) and fibroblasts (Fig. 4M) indicating that most – if not all – cell types in the axolotl limb will be infectable by ASLV-A-pseudotyped retroviruses should they express TVA.

Vascular endothelial cell-specific retroviral infections

We next sought to demonstrate that TVA-dependent control of viral host range could be used to target infections to specific cell types. The role of the vascular system in limb regeneration has not been explored extensively, and we were particularly interested in the potential role of the vascular endothelial cells, as activation of these cells is crucial for angiogenesis (recently reviewed by Chung and Ferrara, 2011). Angiogenesis may be a mechanism by which the regenerating amphibian limb re-establishes its vasculature with the stump, a possibility suggested by experiments in which the vasculature in regenerating salamander limbs is filled with ink (Smith and Wolpert, 1975). Endothelial cell-specific viral infection

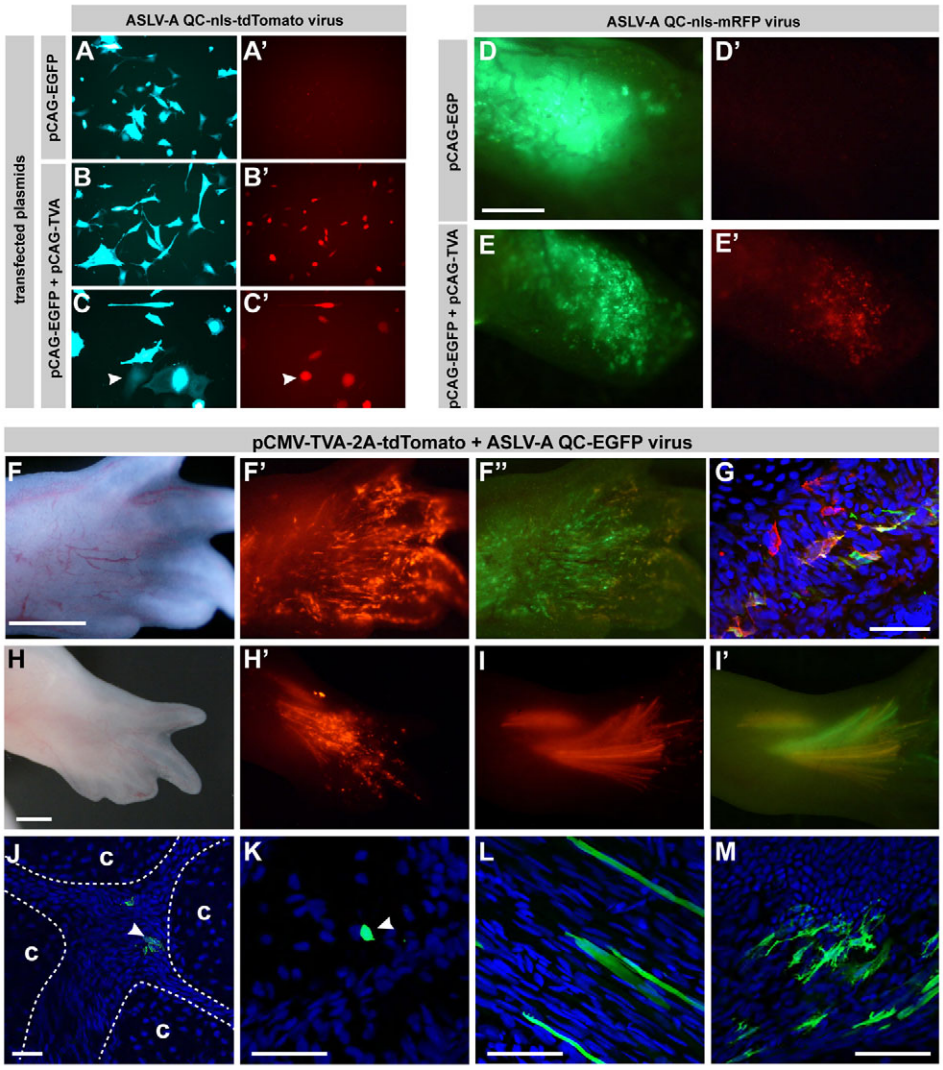

Fig. 4. Axolotl cells ectopically expressing the TVA receptor can be infected by ASLV-A-pseudotyped retroviruses. (**A-B′**) AL1 cells transfected with pCAG-EGFP (control, A,A′) or pCAG-EGFP and pCAG-TVA (B,B′) and exposed ASLV-A-psuedotyped QCMV-nls-tdTomato virus 4 days post-transfection. Cells were imaged live. (A) Green channel shows many transfected control cells. (A′) Red channel shows none of these cells have been infected. (B) Green channel shows many transfected cells. (B′) Red channel with identical imaging conditions as in A′ showing nearly all of the transfected cells have been infected with the virus. (**C**,**C′**) Higher magnification from the same experiment as B showing that cells weakly expressing the co-electroporation marker (arrowheads) can strongly express the viral marker. (**D-E′**) Limbs were electroporated with either pCAG-tdTomato (D,D′) or pCMV-TVA-2A-tdTomato (E,E′) at 1 week post-amputation and injected with ASLV-A pseudotyped QCMV-EGFP 2 days later, and imaged under identical conditions at 4 days post-injection. (D,D′) Without TVA, limbs cannot be infected with the virus (n=8). (E,E′) All limbs (n=8) expressing TVA were infected with the virus. (**F-G**) Late-palette stage regenerating limbs were electroporated with pCMV-TVA-2A-tdTomato, infected with ASLV-A psuedotyped QCMV-EGFP 2 days later, and imaged 4 days post-infection. (G) The limb shown in F-F″ was fixed, sectioned, counterstained with DAPI and percentage of tdTomato$^+$ cells that were also EGFP$^+$ was calculated to be ~80% (n=221/277). (**H-I′**) An electroporation/viral infection experiment was followed until limbs were completely regenerated (n=6). (**J-M**) Examples of EGFP-expressing cells in TVA-expressing/ASLV-A-psuedotyped QCMV-EGFP infected regenerated limbs. (J) 'c' denotes condensed wrist cartilage elements, outlines of which are indicated by dashed lines. Blue is DAPI. Joint cells (arrowhead) are sandwiched between cartilage elements and are more densely packed than surrounding cartilage. (K) Labeled chondrocyte (arrowhead). (L) Labeled muscle fibers. (M) Labeled fibroblasts. Scale bars: 500 μm in D-E′; 1 mm in F-F″,H-I′; 50 μm in G; 100 μm in J-M.

would allow both lineage relationships and gene function studies to be carried out in this context. In a preliminary screen using electroporation of various EGFP-encoding constructs into blastemas, a PECAM (platelet and endothelial cell adhesion molecule, also known as CD31) promoter that is specific to vascular endothelial cells in mice (Kearney et al., 2004) appeared active in axolotls. Hence, we injected single-cell axolotl embryos with this plasmid to generate transgenic F_0 animals. Though embryos were injected when they were single cells, transgenics show mosaic expression of transgenes (Monaghan and Maden, 2012; Sobkow et al., 2006; Whited et al., 2012) that is likely to be due to integration of the transgenic element into the genome after cell division has commenced; we observed a similar phenomenon. EGFP fluorescence was evident in embryos within 5-6 days post-injection. By 10 days, some embryos expressed EGFP within this vasculature of the gills (Fig. 5A,A′). Approximately 100 embryos were injected,

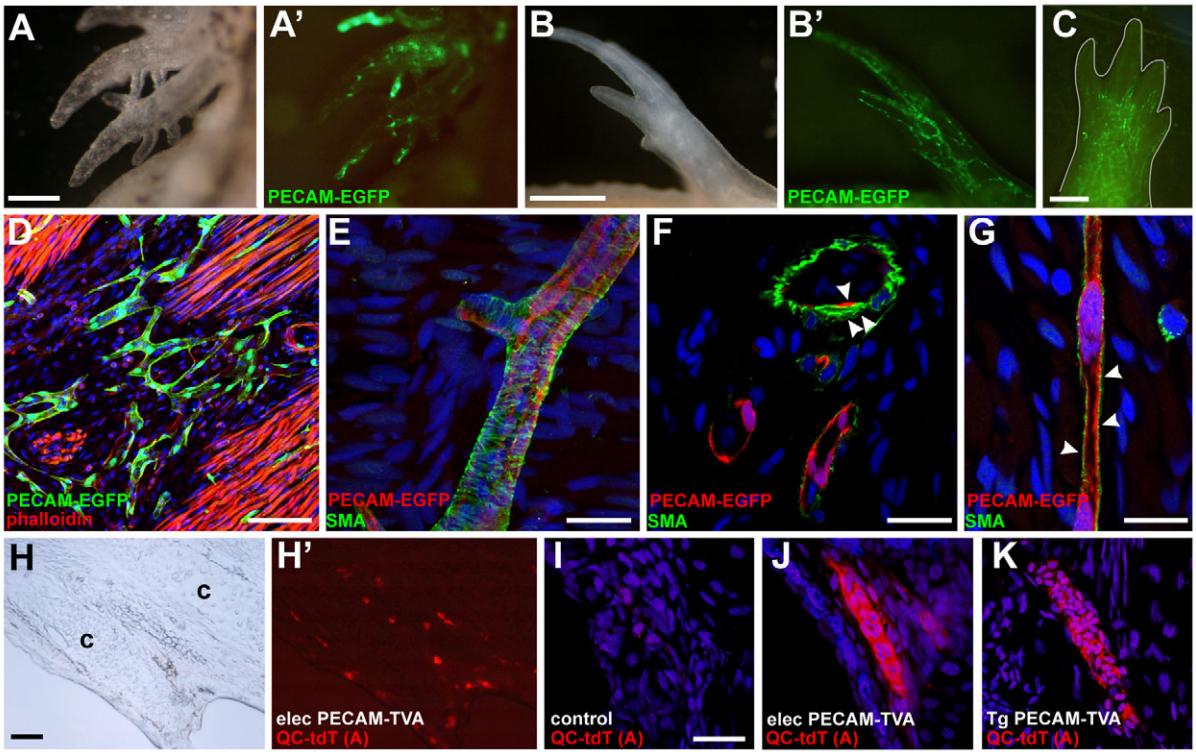

Fig. 5. The TVA/ASLV-A system can be used to target specific cell types in regenerating limbs. (**A-B′**) The mammalian PECAM enhancer/promoter element drives expression of marker genes in vascular endothelial cells in F_0 transgenic axolotls. Bright-field (A) and fluorescent (A′) images of gills and vasculature in a live animal 10 days post-fertilization. Bright-field (B) and fluorescent (B′) images of limb vasculature in a separate live animal 7 weeks post-fertilization. (**C**) $EGFP^+$ vessels in newly regenerated limb (limb outlined). (D-G) Confocal images of F_0 transgenic PECAM-EGFP adult limb 9 weeks post-amputation. (**D**) Section stained with anti-GFP (green), phalloidin (red) and DAPI (blue). (E-G) Sections stained with anti-EGFP expression (red) showing expression in vascular endothelial cells, and cells expressing smooth muscle actin (green). (**E**) Large vessel showing the endothelial cells are ensheathed by smooth muscle actin-expressing cells. (**F**) Vessels in cross-section. Red staining (arrowhead) is luminal to green (double arrowheads). (**G**) Capillary (arrowheads) in longitudinal section. Red staining is luminal to green. (**H**,**H′**) Blastemas were electroporated with pPECAM-TVA (titer 10^8) and infected with ASLV-A-psuedotyped QCMV-tdTomato 3 days post-electroporation. Fully regenerated limbs were fixed and cryosectioned. (H) Bright-field image showing cartilage elements (c) of two adjacent digits. (H′) Red channel reveals tdTomato-expressing cells could be detected among the vasculature between the epidermis and cartilage in the regenerated limbs. (**I-K**) Confocal images showing specific expression of tdTomato in the vasculature of animals expressing TVA from the PECAM promoter who have been infected with ASLV-A-pseudotyped QCMV-tdTomato. Regenerated limbs were fixed, cryosectioned and stained with DAPI. (I) Uninfected animal not expressing TVA shows no fluorescent vessels in the vessel-rich area of the digits between cartilage and epidermis. (J) Using the same imaging conditions, red fluorescent vessels are apparent in the same region of a regenerated limb whose blastema was electroporated with pPECAM-TVA and infected with ASLV-A-pseudotyped QCMV-tdTomato, red fluorescent vessels are apparent. (K) A similar result was obtained by infecting blastemas in PECAM-TVA F_0 transgenic limbs. Scale bars: 500 μm in A-B′; 1 mm in C; 200 μm in D; 50 μm in E,F,I-K; 32 μm in G; 100 μm in H,H′.

34 survived to 7 weeks of development when they were all examined for EGFP fluorescence and 14/32 had EGFP expression characteristic of vascular endothelial cells. We observed EGFP expression in limb vasculature of some juveniles (Fig. 5B,B′), indicating this could be a fruitful means of marking vascular endothelial cells and following their fates over limb regeneration. We amputated this particular limb at a later time (5 months old) and found $EGFP^+$ vessels apparent in the regenerating limb (Fig. 5C, 1 month post-amputation). To verify that the PECAM promoter was specific for vascular endothelial cells, we harvested a regenerating adult limb (9 weeks post-amputation) from the animal depicted in Fig. 5B,C. Cryosections counterstained with phalloidin revealed the architecture of the tissues and the location/shape of EGFP-expressing cells (Fig. 5D) to be consistent with vasculature. We stained sections with an antibody to α-smooth muscle actin (conjugated to FITC, hence we amplified the EGFP signal using a Cy3-conjugated secondary antibody), which is known to be expressed by the cells surrounding vascular endothelial cells and found that, indeed, cells expressing the marker from the PECAM promoter were surrounded by smooth muscle actin-expressing cells (Fig. 5E-G).

Having identified a promoter that is capable of directing gene expression specifically in vascular endothelial cells, we examined whether we could target vascular endothelial cells with ASLV-A-pseudotyped retrovirus by using this element to drive TVA receptor expression. We cloned TVA downstream of the PECAM promoter to create pPECAM-TVA. We reasoned that as PECAM-EGFP F_0 transgenics appear to re-express EGFP from the PECAM promoter during limb regeneration (Fig. 5C), we could introduce pPECAM-TVA during limb regeneration and possibly render the cells infectible by ASLV-A viruses. Following electroporation of pPECAM-TVA into mid-bud staged regenerating limbs, we infected limbs with ASLV-A-psuedotyped QC-tdTomato virus (3 days post-electroporation, 10^8 titer in mammalian cells) and allowed the limbs

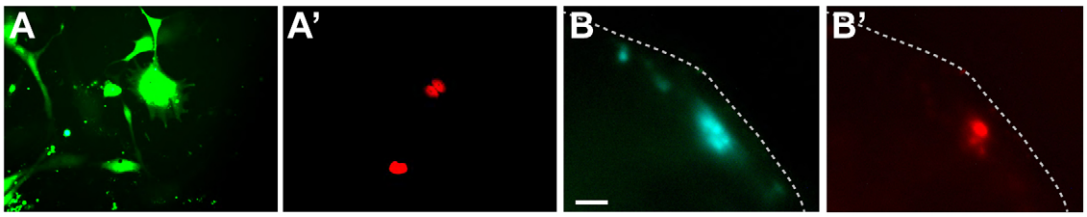

Fig. 6. Expression of Cre recombinase from QC infections in axolotl cells. (**A**,**A′**) Cre-encoding elements delivered to AL1 cells in culture via the VSV-pseudotyped QCAG-Cre retrovirus can catalyze recombination between LoxP sites. AL1 cells were transfected with pCLESLT (transfected cells are green in E) and subsequently infected with QCAG-Cre. (A) Transfected cells express EGFP. (A′) A subset of pCLESLT-expressing cells underwent recombination at the LoxP sites enabling expression of nuclear tdTomato (arrowheads). (**B**,**B′**) Regenerating limbs electroporated with pCLESLT and subsequently infected with QCAG-Cre also show a subset of electroporated cells express tdTomato. Scale bar: 100 μm.

to finish regenerating (harvested 7 weeks post-amputation). As expected, we indeed detected tdTomato^{+} cells among the vasculature in the fully regenerated limb (Fig. 5H,H′, *n*=6/8 limbs). Under these conditions, we did not detect any other labeled cell types. To exclude the possibility of autofluorescence, we imaged the vessel-rich region in the digit tip under the confocal microscope in unmanipulated animals (Fig. 5I) compared with the electroporated and infected animals (Fig. 5J). Because of the caveats associated with electroporation, we anticipate that the best use of the ASLV-A/TVA method will be in a transgenic setting. Hence, we also generated transgenic axolotls with the PECAM-TVA construct. Ultimately, identification of individuals carrying the PECAM-TVA transgene in the germline in which no promiscuous expression is observed would allow the establishment of a line of animals in which only the vasculature can be infected with an ASLV-A-pseudotyped QC virus transducing any gene of interest. Owing to the long generation time of the axolotl, however, we decided to test the system here in transient F_0 animals. These limbs were infected with the same ASLV-A-pseudotyped QC-tdTomato at 3 weeks post-amputation, and tdTomato-expressing cells were apparent only in the vasculature (Fig. 5K, *n*=3/4 limbs). In both electroporation and transgenic experiments, patches of infected vascular endothelial cells comprised a relatively small number of cells (~10-20 cells), probably owing to both the mosaic nature of the TVA expression and the relatively late exposure to the virus – whereby cells divided only a handful of times before limb regeneration was essentially complete – or to the sectioning procedure, which cuts apart vessels as they undulate in and out of the knife plane.

Delivering Cre-encoding elements with retroviruses

We also explored the possibility that viral vectors could be adapted as a triggering mechanism for activating transgenes at specific times during regeneration, encoding Cre recombinase to cells harboring a Cre-dependent transgene. We built a Cre-responsive reporter that is functional in AL1 cells and blastemas, pCAG-loxP-EGFP-3xSTOP-loxP-nls-tdTomato (‘pCLESLT’). In the absence of Cre, cells with the reporter only express EGFP. When co-transfected with a plasmid encoding a constitutively active Cre, AL1 cells and limb blastemas express tdTomato because the floxed EGFP-stop cassette has been eliminated through recombination at the LoxP sites (Whited et al., 2012). Al1 cells transfected with the Cre reporter plasmid were infected with a VSV-pseudotyped QCAG-Cre virus (titer 10^8) 3 days later. We observed expression of tdTomato in a subset of transfected cells (25%, *n*=10/40) only following administration of the virus (Fig. 6A,A′). A similar experiment was performed on regenerating limbs by electroporating the pCLESLT reporter and infecting with VSV-pseudotyped QCAG-Cre virus the following day (Fig. 6B,B′, imaged 2 weeks post-infection). Limbs electroporated with the reporter alone expressed only EGFP (*n*>30); however, electroporated limbs that were subsequently infected with QCAG-Cre always showed a subset of cells expressing tdTomato (*n*=6/6), evidence that Cre expressed from the integrated viral genome is capable of catalyzing recombination at LoxP sites *in vivo* in the axolotl.

DISCUSSION

The primary finding of this work is that pseudotyped murine retroviruses can be used to infect axolotl tissues *in vivo* and elicit robust gene expression. We also show that this infection can be targeted to a specific cell type in conjunction with tissue-specific expression of the TVA receptor and pseudotyping of the virus. This strategy may be a powerful means to irreversibly mark mitotically active cells in axolotls and track their descendants, allowing for lineage tracking during development and regeneration. In theory, this approach can be used to direct the TVA receptor to any cell type of interest in transgenic axolotls (given the appropriate cell type-specific promoter), and such transgenic animals provide a substrate for efficient infection with ASLV-A-pseudotyped QC viruses transducing any gene of interest. In particular, our experiments demonstrate that accessing axolotl vascular endothelial cells is possible with the heterologous PECAM promoter. Although in our initial experiments the labeled cells we observed were all endothelial cells, we cannot rule out the possibility that with the electroporation technique some non-endothelial cells could express the receptor construct in a promiscuous fashion and hence could become infected. However, in a transgenic setting, we never see cells labeled that are not endothelial cells. Future F_1 PECAM-EGFP and PECAM-TVA animals may be valuable for directly assessing the role of vascular endothelial cells during blood vessel regeneration, for example if revascularization occurs solely by angiogenesis and if transdifferentiation to another cell type occurs. A similar technology can also be imagined for other cell types, inching the toolkit available in axolotls closer to that available in more sophisticated model systems such as zebrafish and mice. Although the tissue-specific TVA system could provide a useful modularity, directly cloning cell type-specific promoters into the retroviruses might also be a feasible way of targeting expression to particular cell types (the PECAM promoter is too large for this strategy).

Besides limbs, we have also shown that embryos infected with QC retroviruses develop into juveniles with labeled cells of various types consistent with the time and place of injection. Although this is an important first step for demonstrating the possible utility of

these viruses in contexts where precise embryonic fate maps have not yet been established, further technique refinement might be necessary. We did not, for example, make an attempt to target solely the neural crest cells and assay for the spread of the injection mixture to other nearby locations, although more precise infections might be feasible. Infections of limb buds might also be feasible; if so, this route might be a fruitful way to generate limbs with cells that are genetically different from the rest of the animal, which could bypass deleterious effects that might occur if the element were introduced earlier or more broadly, for example, in standard transgenesis.

We used the QC retroviruses to query which types of progenitor cells are present and mitotically active in the blastema at various time points post-amputation, and we found marked descendant cells of nearly every type (except vasculature, which was labeled only in later infections, and epidermis, which was never labeled) in the regenerated limb for every time point examined. This suggests that not only is the blastema a heterogeneous mixture of potentially lineage-restricted progenitor cells, but that these types of progenitors co-exist, not just in space, but also in time. Hence, it is unlikely that, for example, a wave of muscle-specific progenitors populate the whole blastema at one time point, chondrocytic progenitors at another time point, etc. Interestingly, however, the relative proportions of these progenitors shift over time. In the latest infections, the most commonly labeled cells were in the muscle lineage, whereas connective tissue lineages are labeled to a greater extent in early blastemas than in later blastemas. This pattern is also seen with chondrocytes. These differences could reflect differences in the timing of differentiation of different lineages, for example chondrocytes differentiating sooner and having decreased viral accessability after condensation and/or muscle precursor cells remaining mitotically active longer than other progenitors. As it seems that most progenitor cell types are simultaneously recruited into the blastema, the issue of whether distinct or overlapping signaling pathways draw them there becomes pressing. Identifying the signaling pathways that are activated following amputation may shed light onto how these distinct progenitor cell types are cued to form at essentially the same time, as well as how these processes may converge or diverge from the processes that create a pool of limb progenitors during limb bud development. Our data suggests progenitors may be located near each other in the early blastema yet their descendants in the full regenerate become spatially distinct, similar to conclusions drawn from infections of chick limb buds (Pearse et al., 2007), though this tendency decreases as blastemas mature, and when clones were sparse (for example, a single progenitor may have been infected), usually a single clump of the same cells were detected in the regenerate. Future versions of the viruses designed for precise lineage mapping may help resolve lineage relationships.

The only cell type whose progenitors were not labeled at every time point assayed was the vasculature, which was not labeled in regenerates infected at 3 days post-amputation. By contrast, labeled vascular cells were readily detected in infections at 7 days post-amputation, after which their numbers waned and were relatively small by 3 weeks post-amputation. These results are both consistent with electroporation (J.L.W. and C.J.T., unpublished), as well as the previously described vasculature in regenerating newt and axolotl limbs (Smith and Wolpert, 1975). However, the initial exclusion of the vasculature has since been challenged by another study that detected small capillaries connected to stump vasculature as early as 7 days post-amputation in newts (Rageh et al., 2002). Our results indeed point to an early stage where the forming blastema is likely to be avascular, drawing an interesting similarity between the nascent blastema and the avascular region beneath the apical epidermal ridge in the developing limb bud (Evans, 1909).

Our experiments also show that retroviruses can be used to misexpress a factor with functional consequences to the regenerating limb. The defects in QCAG-SHH-infected limbs are consistent with defects observed when regenerating axolotl limbs were infected with SHH-encoding Vaccinia (Roy et al., 2000), though in the Vaccinia study ectopic digits were also observed. Differences between expression level/number of infected cells and timing of ectopic SHH expression may account for the difference. Ectopic expression of SHH from a chondrocyte-specific promoter in transgenic mice leads to carpal and tarsal joint separation defects (Tavella et al., 2006), and as chondrocyte progenitors are readily infected by the QC viruses, a similar defect may have occurred here.

In summary, we have demonstrated that the QC retroviruses are a powerful means of labeling axolotl cells *in vivo*. We anticipate that this technology will fill a void in the axolotl research community for robust – yet reasonably fast – analysis of both cell fate and gene function.

Acknowledgements
We thank Santiago Rompani for virus help; Melissa Werner and Brian Martineau for animal husbandry; Stephane Roy for AL1 cells; and Josh Gross, Christina DeMaso, Natalia Surzenko, Jonathan Tang and Johanna Kowalko for advice.

Funding
This work was supported by the National Institutes of Health [F32HD054082 to J.L.W., and R21AR059884 and R01HD045499 to C.J.T.], by MIT Undergraduate Research Opportunities Program (S.L.T.) and by the Howard Hughes Medical Institute (K.T.B. and C.L.C.). Deposited in PMC for release after 6 months.

Competing interests statement
The authors declare no competing financial interests.

Supplementary material
Supplementary material available online at
http://dev.biologists.org/lookup/suppl/doi:10.1242/dev.087734/-/DC1

References

Atkinson, D. L., Stevenson, T. J., Park, E. J., Riedy, M. D., Milash, B. and Odelberg, S. J. (2006). Cellular electroporation induces dedifferentiation in intact newt limbs. *Dev. Biol.* **299**, 257-271.
Beier, K. T., Samson, M. E., Matsuda, T. and Cepko, C. L. (2011). Conditional expression of the TVA receptor allows clonal analysis of descendents from Cre-expressing progenitor cells. *Dev. Biol.* **353**, 309-320.
Berg, D. A., Kirkham, M., Beljajeva, A., Knapp, D., Habermann, B., Ryge, J., Tanaka, E. M. and Simon, A. (2010). Efficient regeneration by activation of neurogenesis in homeostatically quiescent regions of the adult vertebrate brain. *Development* **137**, 4127-4134.
Brockes, J. P. and Kumar, A. (2005). Appendage regeneration in adult vertebrates and implications for regenerative medicine. *Science* **310**, 1919-1923.
Burns, J. C., Matsubara, T., Lozinski, G., Yee, J. K., Friedmann, T., Washabaugh, C. H. and Tsonis, P. A. (1994). Pantropic retroviral vector-mediated gene transfer, integration, and expression in cultured newt limb cells. *Dev. Biol.* **165**, 285-289.
Cash, D. E., Gates, P. B., Imokawa, Y. and Brockes, J. P. (1998). Identification of newt connective tissue growth factor as a target of retinoid regulation in limb blastemal cells. *Gene* **222**, 119-124.
Chung, A. S. and Ferrara, N. (2011). Developmental and pathological angiogenesis. *Annu. Rev. Cell Dev. Biol.* **27**, 563-584.
Echeverri, K. and Tanaka, E. M. (2002). Ectoderm to mesoderm lineage switching during axolotl tail regeneration. *Science* **298**, 1993-1996.
Echeverri, K. and Tanaka, E. M. (2003). Electroporation as a tool to study in vivo spinal cord regeneration. *Dev. Dyn.* **226**, 418-425.
Echeverri, K. and Tanaka, E. M. (2005). Proximodistal patterning during limb regeneration. *Dev. Biol.* **279**, 391-401.
Epperlein, H., Meulemans, D., Bronner-Fraser, M., Steinbeisser, H. and Selleck, M. A. (2000). Analysis of cranial neural crest migratory pathways in axolotl using cell markers and transplantation. *Development* **127**, 2751-2761.

Evans, H. M. (1909). On the earliest blood-vessels in the anterior limb buds of birds and their relation to the primary subclavian artery. *Am. J. Anat.* **9**, 281-319.
Federspiel, M. J., Bates, P., Young, J. A., Varmus, H. E. and Hughes, S. H. (1994). A system for tissue-specific gene targeting: transgenic mice susceptible to subgroup A avian leukosis virus-based retroviral vectors. *Proc. Natl. Acad. Sci. USA* **91**, 11241-11245.
Hanken, J. and Gross, J. B. (2005). Evolution of cranial development and the role of neural crest: insights from amphibians. *J. Anat.* **207**, 437-446.
Kawakami, Y., Rodriguez Esteban, C., Raya, M., Kawakami, H., Martí, M., Dubova, I. and Izpisúa Belmonte, J. C. (2006). Wnt/beta-catenin signaling regulates vertebrate limb regeneration. *Genes Dev.* **20**, 3232-3237.
Kearney, J. B., Kappas, N. C., Ellerstrom, C., DiPaola, F. W. and Bautch, V. L. (2004). The VEGF receptor flt-1 (VEGFR-1) is a positive modulator of vascular sprout formation and branching morphogenesis. *Blood* **103**, 4527-4535.
Kragl, M., Knapp, D., Nacu, E., Khattak, S., Maden, M., Epperlein, H. H. and Tanaka, E. M. (2009). Cells keep a memory of their tissue origin during axolotl limb regeneration. *Nature* **460**, 60-65.
Kumar, A., Velloso, C. P., Imokawa, Y. and Brockes, J. P. (2000). Plasticity of retrovirus-labelled myotubes in the newt limb regeneration blastema. *Dev. Biol.* **218**, 125-136.
Kumar, A., Godwin, J. W., Gates, P. B., Garza-Garcia, A. A. and Brockes, J. P. (2007). Molecular basis for the nerve dependence of limb regeneration in an adult vertebrate. *Science* **318**, 772-777.
Lévesque, M., Gatien, S., Finnson, K., Desmeules, S., Villiard, E., Pilote, M., Philip, A. and Roy, S. (2007). Transforming growth factor: beta signaling is essential for limb regeneration in axolotls. *PLoS ONE* **2**, e1227.
Lewis, B. C., Chinnasamy, N., Morgan, R. A. and Varmus, H. E. (2001). Development of an avian leukosis-sarcoma virus subgroup A pseudotyped lentiviral vector. *J. Virol.* **75**, 9339-9344.
Lois, C., Hong, E. J., Pease, S., Brown, E. J. and Baltimore, D. (2002). Germline transmission and tissue-specific expression of transgenes delivered by lentiviral vectors. *Science* **295**, 868-872.
Mercader, N., Tanaka, E. M. and Torres, M. (2005). Proximodistal identity during vertebrate limb regeneration is regulated by Meis homeodomain proteins. *Development* **132**, 4131-4142.
Monaghan, J. R. and Maden, M. (2012). Visualization of retinoic acid signaling in transgenic axolotls during limb development and regeneration. *Dev. Biol.* **368**, 63-75.
Niwa, H., Yamamura, K. and Miyazaki, J. (1991). Efficient selection for high-expression transfectants with a novel eukaryotic vector. *Gene* **108**, 193-199.
Pearse, R. V., 2nd, Scherz, P. J., Campbell, J. K. and Tabin, C. J. (2007). A cellular lineage analysis of the chick limb bud. *Dev. Biol.* **310**, 388-400.
Rageh, M. A., Mendenhall, L., Moussad, E. E., Abbey, S. E., Mescher, A. L. and Tassava, R. A. (2002). Vasculature in pre-blastema and nerve-dependent blastema stages of regenerating forelimbs of the adult newt, Notophthalmus viridescens. *J. Exp. Zool.* **292**, 255-266.
Rapaport, D. H., Wong, L. L., Wood, E. D., Yasumura, D. and LaVail, M. M. (2004). Timing and topography of cell genesis in the rat retina. *J. Comp. Neurol.* **474**, 304-324.
Roy, S., Gardiner, D. M. and Bryant, S. V. (2000). Vaccinia as a tool for functional analysis in regenerating limbs: ectopic expression of Shh. *Dev. Biol.* **218**, 199-205.
Sidman, R. L. (1961). Histogenesis of mouse retina studied with thymidine-H^3. In *The Structure of the Eye* (ed. G. K. Smelser), pp. 487-507. New York, NY: Academic Press.
Smith, A. R. and Wolpert, L. (1975). Nerves and angiogenesis in amphibian limb regeneration. *Nature* **257**, 224-225.
Sobkow, L., Epperlein, H. H., Herklotz, S., Straube, W. L. and Tanaka, E. M. (2006). A germline GFP transgenic axolotl and its use to track cell fate: dual origin of the fin mesenchyme during development and the fate of blood cells during regeneration. *Dev. Biol.* **290**, 386-397.
Tavella, S., Biticchi, R., Morello, R., Castagnola, P., Musante, V., Costa, D., Cancedda, R. and Garofalo, S. (2006). Forced chondrocyte expression of sonic hedgehog impairs joint formation affecting proliferation and apoptosis. *Matrix Biol.* **25**, 389-397.
Whited, J. L. and Tabin, C. J. (2009). Limb regeneration revisited. *J. Biol.* **8**, 5.
Whited, J. L., Lehoczky, J. A., Austin, C. A. and Tabin, C. J. (2011). Dynamic expression of two thrombospondins during axolotl limb regeneration. *Dev. Dyn.* **240**, 1249-1258.
Whited, J. L., Lehoczky, J. A. and Tabin, C. J. (2012). Inducible genetic system for the axolotl. *Proc. Natl. Acad. Sci. USA* **109**, 13662-13667.
Young, R. W. (1985a). Cell differentiation in the retina of the mouse. *Anat. Rec.* **212**, 199-205.
Young, R. W. (1985b). Cell proliferation during postnatal development of the retina in the mouse. *Brain Res.* **353**, 229-239.
Young, J. A., Bates, P. and Varmus, H. E. (1993). Isolation of a chicken gene that confers susceptibility to infection by subgroup A avian leukosis and sarcoma viruses. *J. Virol.* **67**, 1811-1816.
Yu, S. F., von Rüden, T., Kantoff, P. W., Garber, C., Seiberg, M., Rüther, U., Anderson, W. F., Wagner, E. F. and Gilboa, E. (1986). Self-inactivating retroviral vectors designed for transfer of whole genes into mammalian cells. *Proc. Natl. Acad. Sci. USA* **83**, 3194-3198.